



Middepth spreading in the subpolar North Atlantic Ocean: Reconciling CFC-11 and float observations

E. Kvaleberg,^{1,2} T. W. N. Haine,¹ and D. W. Waugh¹

Received 16 January 2007; revised 24 December 2007; accepted 10 March 2008; published 9 August 2008.

[1] Chlorofluorocarbons (CFCs) enter the middepth layers of the North Atlantic Ocean from the atmosphere during the formation of dense mode water in the Labrador and Irminger Seas of the subpolar gyre. The CFC-bearing waters then spread from the convection regions through advection and diffusion of the water masses. Using recent estimates of the circulation at 1500 m depth from subsurface profiling floats the spreading of CFC-11 is simulated in the subpolar North Atlantic with an advective-diffusive model. Several numerical experiments are performed with different stream functions, lateral diffusivities and variations in the CFC-11 sources. The results are then compared to the observed CFC-11 field during 1996–1998. Poor fits are found for diffusivities less than about $500 \text{ m}^2 \text{ s}^{-1}$. Better fits are found for diffusivities ranging from 500 – $12,000 \text{ m}^2 \text{ s}^{-1}$, although unrealistically smooth model solutions are produced if the diffusivity exceeds about $3000 \text{ m}^2 \text{ s}^{-1}$. Simulations that include both Labrador and Irminger Sea CFC-11 sources fit the data better than with Labrador sources alone. None of the model CFC solutions fit the data within the CFC uncertainty over the whole domain; the model performs well in the western part of the subpolar gyre, but CFC-11 concentrations are consistently too low in the West European Basin. It is possible that uncertainty in the float-based circulation can account for these misfits, and a more accurate circulation estimate might be able to fit the observed CFC-11 field. Alternatively, time variations in the flow or deep water formation processes, which clearly exist in the real ocean, may need to be included.

Citation: Kvaleberg, E., T. W. N. Haine, and D. W. Waugh (2008), Middepth spreading in the subpolar North Atlantic Ocean: Reconciling CFC-11 and float observations, *J. Geophys. Res.*, *113*, C08019, doi:10.1029/2007JC004104.

1. Introduction

[2] The subpolar North Atlantic Ocean is of critical importance for regional and global climate. Vigorous air-sea interaction cools and freshens warm, salty subtropical waters as they flow northeast in the North Atlantic Current. The net buoyancy loss causes deep-reaching convection and formation of large volumes of nearly homogeneous water that spread out at intermediate and deep levels throughout the North Atlantic and beyond. These water masses are collectively known as subpolar mode water [Talley and McCartney, 1982]. The coldest mode water is formed in the Labrador Sea (Labrador Seawater, LSW), although there is also evidence that it is formed, intermittently, in the Irminger Sea at the end of stormy winters with positive values of the North Atlantic Oscillation (NAO) index [Pickart et al., 2003].

[3] Spreading of LSW can be traced in three principal paths at, nominally, 1000–2000 m depth (vertical current

shear in the weakly-stratified LSW is small; Talley and McCartney [1982]; Schmitz and McCartney [1993]). First, there is relatively fast cyclonic recirculation in the Labrador, Irminger, and Newfoundland basins. Second, there is spreading into the eastern basin, probably steered through deep gaps in the Mid-Atlantic Ridge such as the Charlie-Gibbs Fracture Zone. Finally, LSW escapes south past the Grand Banks into the southbound Deep Western Boundary Current and hence into the upper layers of the North Atlantic Deep Water, a principal component in the global Meridional Overturning Circulation [Schmitz, 1995].

[4] This picture has been largely confirmed by recent results on the time-averaged middepth circulation in the subpolar North Atlantic Ocean from subsurface floats released during 1996–2003 [see Lavender et al., 2000; Fischer and Schott, 2002; Faure and Speer, 2005, and references therein]. The large scale circulation is dominated by the cyclonic boundary current, rounding Greenland and proceeding south along the coast of Labrador. Interestingly, previously unknown subbasin scale recirculations have been identified in the Labrador and Irminger Seas. The most recent work has synthesized all available float displacement data to produce a coherent, basin-wide, gridded mean velocity field at the nominal spreading depth of LSW [Faure and Speer, 2005, Figure 7a]. The stream function is shown in Figure 1a and represents, arguably, the most

¹Department of Earth and Planetary Sciences, Johns Hopkins University, Baltimore, Maryland, USA.

²Norwegian Naval Training Establishment, Tactics and Doctrine/METOC, Bergen, Norway.

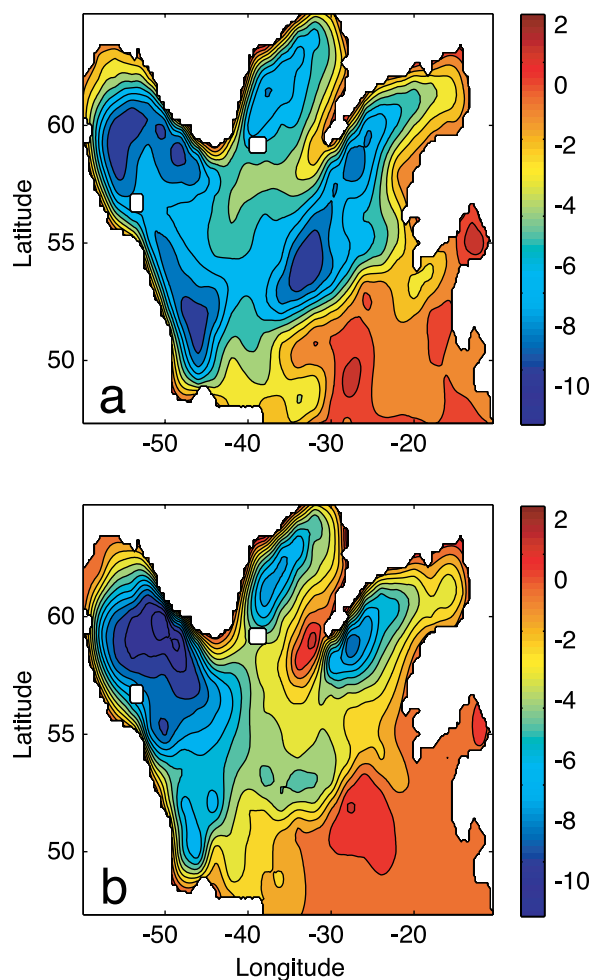


Figure 1. (a) Unconstrained mean float-derived geostrophic stream function (cm) for, nominally, 1996–2003 at 1500–1750 m depth. The white squares indicate the locations where CFC-11 is released in the numerical advective-diffusive model. (b) Float-derived stream function calculated using only the subset of data that is statistically significant, and constrained by isopycnal potential vorticity on the LSW layer. The stream functions were provided by V. Faure [Faure and Speer, 2005].

detailed knowledge of subsurface circulation from the whole global ocean. Faure and Speer [2005] calculated three additional stream functions by imposing various potential vorticity constraints on the mean field. The differences between the three constrained stream functions and the unconstrained field are relatively minor; the principal spreading pathways described above are present in all stream functions, as is the boundary current system in the Irminger and Labrador Seas. The stream function that differs most from the unconstrained mean field is shown in Figure 1b [Faure and Speer, 2005, Figure 7b].

[5] Rapid diabatic conversion in the winter mixed layers also modifies the dissolved gas content of subpolar mode waters, and hence LSW carries high concentrations of anthropogenic carbon and chlorofluorocarbons (CFCs). Complementary evidence on LSW spreading rates and pathways therefore comes from data on the dispersal of

CFCs through the area. Multiple ship surveys in the period 1996–1998 have allowed gridded maps of middepth subpolar CFC-11 to be prepared [Rhein et al., 2002]. Again, this coverage is unprecedented in its detail (Figure 2).

[6] A natural question is to ask if the circulation data are consistent with the CFC data and known LSW sources. Interannual variability is known to exist in both deep convection intensity [see, e.g., Yashayaev, 2007, and references therein] and in the basin-scale flow [Häkkinen and Rhines, 2004]. There are also various systematic and random errors in the float-based circulation and the CFC maps. It is therefore not obvious that the two data sets can be reconciled. Addressing this question is the aim of this paper. Our approach is to use the float-based velocity field in a two-dimensional advective-diffusive numerical model to simulate the spreading of CFC-11 in the subpolar North Atlantic Ocean. The model results are then compared to the CFC-11 data. We seek the best possible fit between the simulated CFC-11 field and the observations. Then we ask what constraints, if any, are placed on the horizontal eddy diffusion coefficient, on the sources of CFC, and hence on the sources of LSW.

2. Data and Methods

[7] We use the MIT general circulation model (MITgcm; Marshall et al. [1997]), modified to run in a two-dimensional advective-diffusive mode using the velocity fields of Faure and Speer [2005]. The domain is shown in Figure 1 and we neglect any vertical processes. CFC-11 is released in the Labrador Sea and/or the Irminger Sea (white squares in Figure 1). In the Labrador Sea, the source region corresponds to the location of maximum mixed layer depth during convection events, as identified by Pickart et al. [2002, Figure 12d; see also Azetsu-Scott et al., 2005]. In the Irminger Sea, the source region is located east of Cape Farewell, where planetary potential vorticity has a minimum and LSW appears to be sometimes formed [Pickart et al., 2003]. The CFC-11 source concentration is determined by the atmospheric history [Walker et al., 2000], CFC-11

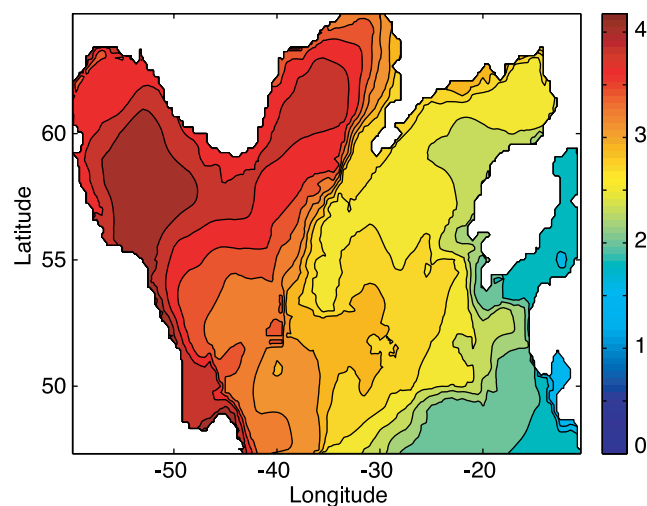


Figure 2. Observed CFC-11 (pmol/l) during, nominally, 1996–1998 at the depth of LSW, around 1500 m, provided by M. Rhein [Rhein et al., 2002].

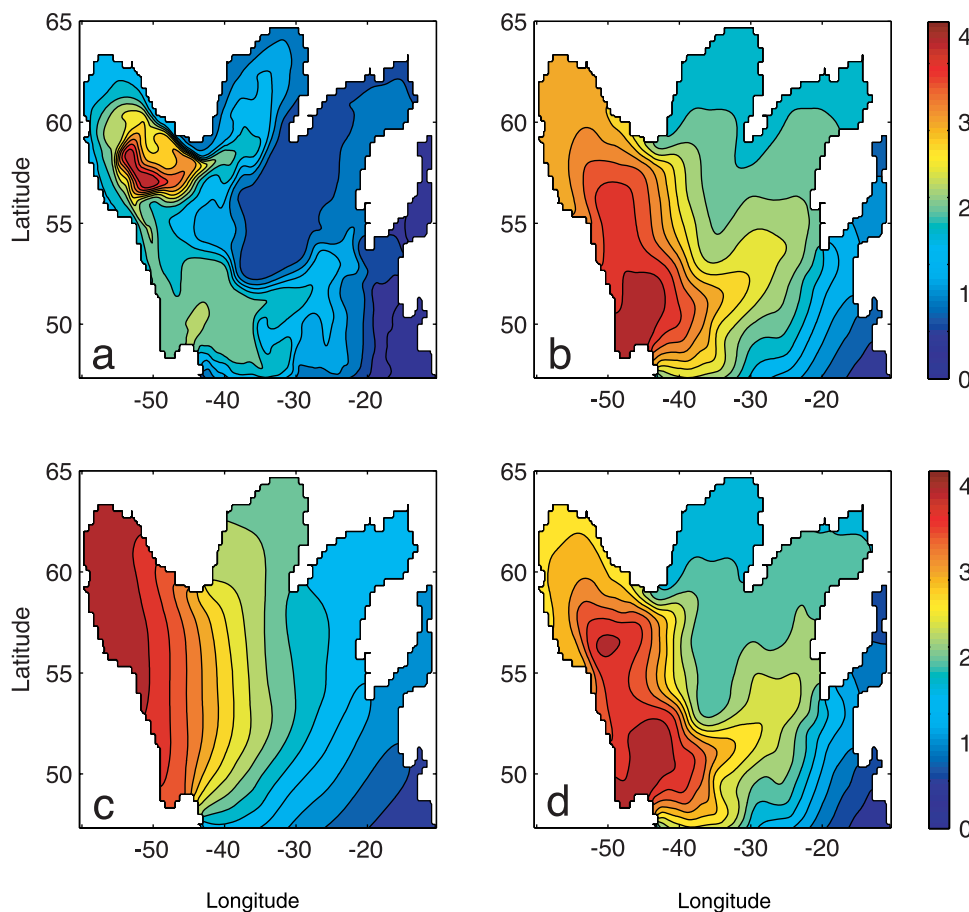


Figure 3. Simulated CFC-11 distributions (pmol/l) with a source in the Labrador Sea and diffusivity (a) $100 \text{ m}^2 \text{ s}^{-1}$, (b) $1000 \text{ m}^2 \text{ s}^{-1}$, (c) $5000 \text{ m}^2 \text{ s}^{-1}$, and (d) spatially varying diffusivity from *Straneo et al.* [2003].

solubility [Warner and Weiss, 1985], and a saturation that is allowed to vary between experiments (the final simulated CFC-11 distribution in each experiment is scaled so that the peak model concentration matches the data). The model is run from 1945–1997, then for an additional six months with zero CFC-11 flux so that the sharp CFC-11 maxima within the source regions can be redistributed. The southern boundary is open so that CFC-11 can diffuse out of the domain thereby preventing unrealistic accumulation of CFC-11 there.

[8] There are three sets of numerical experiments distinguished by: (1) a CFC-11 source in the Labrador Sea, (2) a source in the Irminger Sea, and (3) sources in both locations, with the Labrador Sea source always active, and the Irminger Sea source active only when the NAO index is positive. In each set, experiments are run with uniform horizontal (eddy) diffusivities ranging from $50\text{--}12000 \text{ m}^2 \text{ s}^{-1}$. In addition, we also perform experiments with the spatially-varying diffusivity fields used by *Straneo et al.* [2003] (their Figure 3a), modified to fit our model domain.

[9] The float-based stream functions from *Faure and Speer* [2005] are averages during the period 1996–2003, at a depth of 1500–1750 m (nominal resolution 1° latitude by 2° longitude). The first stream function is the unconstrained mean field, while the remaining three are calculated using (1) a barotropic f/h constraint, (2) an isopycnal PV

constraint on the LSW layer, and (3) an isopycnal PV constraint on the LSW layer, and using only the statistically significant float data (about 8% of the available data). The unconstrained mean field and stream function (3) are shown in Figure 1. Stream functions (1) and (2) are very similar to the unconstrained mean field. Further details are given by *Faure and Speer* [2005], and their Figures 6 and 7 in particular. Each of the stream function maps is consistent with the float data and, in a crude way, they represent the uncertainty in the circulation estimate.

[10] Although the boundary currents are clearly present in all four stream functions, uncertainties in boundary current strength are relatively large. The conventional picture [Talley and McCartney, 1982; Schmitz, 1996] shows the boundary current east of Newfoundland as a fast pathway for LSW export from the subpolar gyre. Floats rarely escape south past Flemish Cap and the Grand Banks into the subtropics, however [Fischer and Schott, 2002; Lavender et al., 2000]. Resolution of this apparent contradiction is still pending and it is possible that the float-based velocity field may be substantially biased in this area [see also Getzlaff et al., 2006]. Moreover, considering the whole domain, only about half of the velocity estimates are significant at the 95% confidence level. Uncertainties are large in the interior of the domain, and close to Flemish Cap

Table 1. A Subset of the Numerical Experiments Listed With Corresponding χ^2 Values for the Whole Domain (χ_1^2), and With the South-Eastern Corner Excluded From the Analysis (χ_2^2)^a

Source	Diff.	χ_1^2	χ_2^2	%
Lab	50	140	150	
Lab	500	22	18	16
Lab	1,000	21	19	11
Lab	3,000	23	17	27
Lab	5,000	29	20	32
Lab	12,000	34	23	33
Irm	50	180	180	–
Irm	500	24	14	44
Irm	1,000	8.8	2.5	72
Irm	3,000	8.2	2.5	70
Irm	5,000	8.7	2.5	72
Irm	12,000	8.6	3.3	62
Both	50	120	130	–
Both	500	16	9.0	42
Both	1,000	11	7.3	36
Both	3,000	8.5	4.2	51
Both	5,000	11	4.6	58
Both	12,000	17	9.1	47

^aThe percentage of χ_1^2 that is due to the error in the south-eastern corner is given in the final column (%).

where the high eddy variability leads to poor sampling by the floats.

[11] Our numerical results are compared to the gridded CFC-11 field described by *Rhein et al.* [2002] (Figure 2). CFC-11 data within $27.74 \leq \sigma_\theta \leq 27.80$ obtained during 1996–1998 were gridded using a topography-following interpolation scheme and taken to represent the 1997 LSW CFC field. The uncertainty in the gridded CFC-11 field is estimated to be 5–20%, depending on location, and the nominal resolution is 100–200 km. A small gap in the *Rhein et al.* [2002] gridded data was filled by interpolating the surrounding values. To quantify the comparison between the simulated CFC-11 field and data we calculate chi-square values (χ^2) for each model experiment with the formula $(\mathbf{c}^T \mathbf{A}^{-1} \mathbf{c}) N^{-1}$, where \mathbf{c} is a vector containing the differences ($c_m - c_o$) between the simulated (c_m) and observed (c_o) CFC-11 concentration at each grid point. The number of degrees of freedom, N , is taken as the total number of CFC-11 values and \mathbf{A} is a diagonal matrix of variances in the observed field from *Rhein et al.* [2002, Figure 10a] (estimated using a jackknife procedure). We also include in \mathbf{A} a 5% fractional error to account for instrumental and calibration uncertainties in the CFC data [*Rhein et al.*, 2002]. The resulting uncertainties in the observed CFC-11 field thus range from 9–18%. Statistical consistency between the numerical experiments and observations requires values of χ^2 that are close to 1. In addition, we estimate characteristic CFC-11 spatial scales by calculating correlations as a function of separation for each CFC-11 field.

3. Results

3.1. Labrador Sea CFC-11 Source

[12] Figure 3 shows four experiments with a CFC-11 source in the Labrador Sea and diffusivities of: (1) $100 \text{ m}^2 \text{ s}^{-1}$, (2) $1000 \text{ m}^2 \text{ s}^{-1}$, (3) $5000 \text{ m}^2 \text{ s}^{-1}$, and (4) the spatially-varying diffusivity field. For a diffusivity of $100 \text{ m}^2 \text{ s}^{-1}$ the comparison with the observed CFC-11 field is poor and χ^2

is 100 (compare Figures 2 and 3a). In this case, CFC-11 spreads mostly along the internal recirculation pathways within the Labrador Sea, but the diffusivity is too low to allow sufficient amounts to enter the western boundary current and the advective pathway into the Irminger Sea. The χ^2 values for experiments with uniform diffusivities between $500\text{--}3000 \text{ m}^2 \text{ s}^{-1}$ are all within 21–23 (one example is shown in Figure 3b). In these cases, CFC-11 is transported along the advective pathways, but there is also diffusion across these trajectories into the northern Labrador and Irminger Seas, and into the Iceland Basin across the strong flow along Reykjanes Ridge. With higher diffusivities, 5000 and $12,000 \text{ m}^2 \text{ s}^{-1}$, χ^2 increases to 29 and 34, respectively (Table 1).

[13] Comparison of the simulated CFC-11 fields with the data reveals three areas with large differences (Figure 4). Namely, in the Irminger Sea and in the southeastern corner of the domain the model concentrations are too low, whereas north of Flemish Cap (around 45°W , 50°N), the model concentrations are too high. This latter area coincides with the region of largest uncertainty in both the float-based velocity field and the CFC-11 observations, and it is therefore unsurprising that the comparison is poor here.

3.2. Including an Irminger Sea CFC-11 Source

[14] In the above, a uniform diffusivity between $500\text{--}3000 \text{ m}^2 \text{ s}^{-1}$ gives the lowest χ^2 values compared to observations. Now we change the CFC-11 source in two other sets of experiments, first with active sources in both the Labrador and Irminger Seas, and second with CFC-11 released only in the Irminger Sea (Figure 5). With both sources, the result is better than the experiment with the Labrador Sea source. χ^2 is reduced from 22–23 to 8.5–16 (Table 1), essentially because the error in the Labrador and Irminger Seas has been decreased (Figure 6a). There is still accumulation of CFC-11 north of Flemish cap that is not present in the observations, but in the Labrador Sea and the Iceland Basin the error is comparatively minor.

[15] The case of an Irminger-Sea-only source is unrealistic because the Labrador Sea is clearly a more important

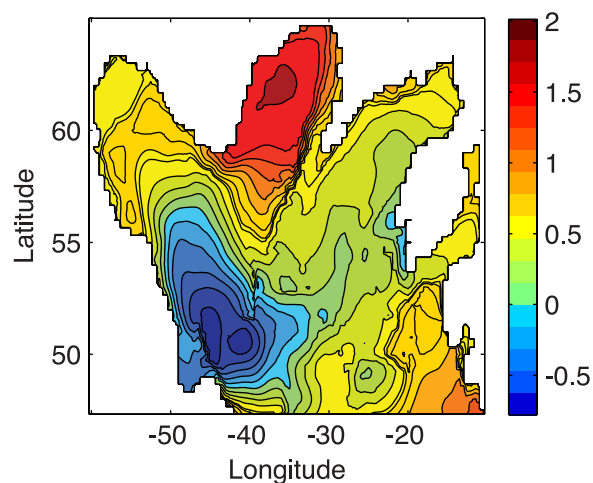


Figure 4. Difference in observed and simulated CFC-11 concentration (pmol/l) for the experiment with a source in the Labrador Sea and a diffusivity of $1000 \text{ m}^2 \text{ s}^{-1}$.

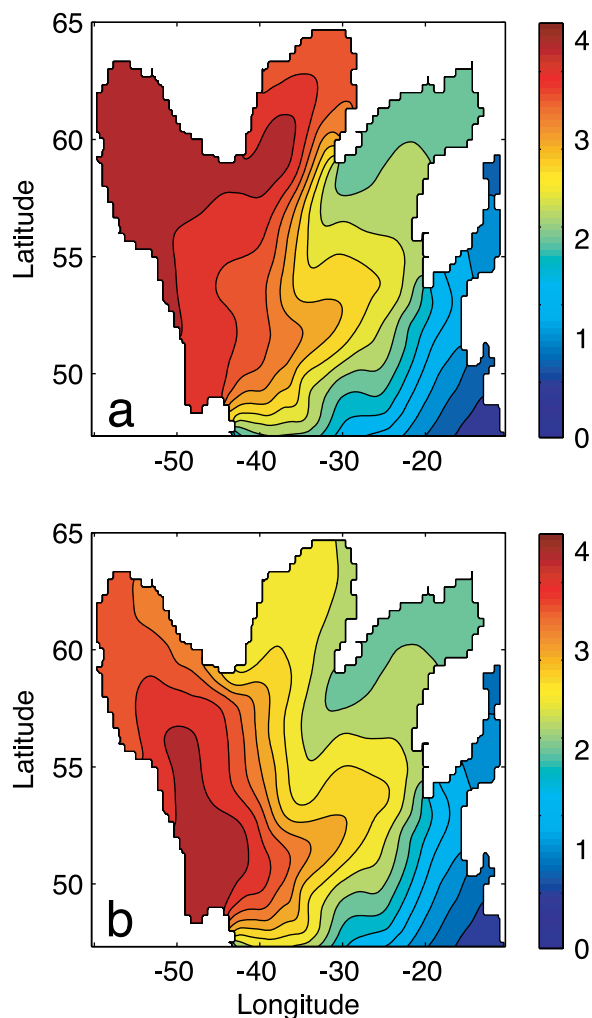


Figure 5. Simulated CFC-11 distributions (pmol/l) with uniform diffusivity ($1000 \text{ m}^2 \text{ s}^{-1}$) and a CFC-11 source in (a) the Irminger Sea, and (b) both the Labrador and Irminger Seas.

source of LSW than the Irminger Sea. Nevertheless, this set of experiments is revealing because it actually gives the best comparison with data ($\chi^2 \approx 8.0$). The source is located at the site of minimum planetary potential vorticity [Pickart *et al.*, 2003, Figure 5], in the trough of a recirculation cell. Some CFC-11 is therefore advected directly back into the Irminger Sea, and some flows into the Labrador Sea and south toward Flemish Cap in the boundary current along the Greenland and Labrador coasts. This process also reduces the amount of CFC-11 retained in the area north of Flemish Cap. The differences between the observed and simulated fields are mainly located along the southern boundary and in the Iceland Basin (Figure 6b).

[16] The model-data misfit in the southeastern corner of the domain is consistently large in most cases. Table 1 lists values of χ^2 for the different experiments, and also χ^2 when CFC-11 concentrations in the southeastern corner is disregarded. Generally, when χ^2 decreases, the contribution to χ^2 from the southeastern corner increases, so that for experiments with χ^2 less than 10, approximately 50–70% of this value is due to the error there. For instance, with only

a source in the Irminger Sea and diffusivities of $1000 \text{ m}^2 \text{ s}^{-1}$, 72% of the value for χ^2 stems from the low CFC-11 concentration in the south-eastern corner of the domain compared to observations.

3.3. Experiments With Different Stream Functions

[17] In the numerical experiments so far we have simulated the spreading of CFC-11 with the unconstrained mean stream function of *Faure and Speer* [2005], with variations in the sources and diffusivity. The best comparison with observations were found for a diffusivity of approximately $1000 \text{ m}^2 \text{ s}^{-1}$, and we use this value in additional experiments with the constrained stream functions described in the previous section. With a CFC-11 source in both the Labrador and Irminger Seas, the values of χ^2 are 18 (barotropic f/h constraint), 35 (isopycnal PV constraint on the LSW layer), and 39 (corresponding to the stream function calculated using only the statistically significant float data). With the unconstrained mean stream function, $\chi^2 = 11$. Similarly, if there is only CFC-11 release in the Irminger Sea, χ^2 increases to 25, 40, and 53, as opposed to $\chi^2 = 8.8$ with the unconstrained mean stream function. Two examples are shown in Figure 7.

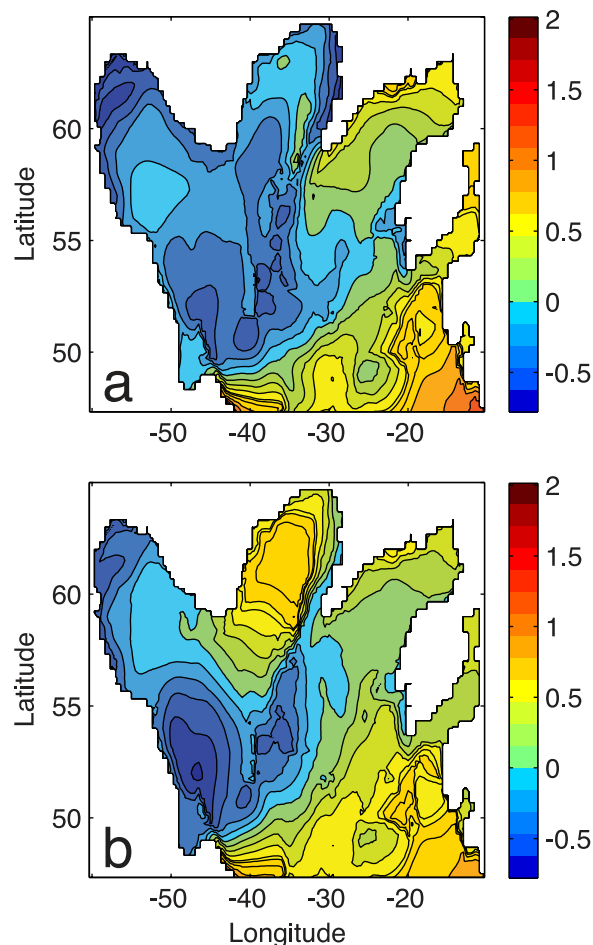


Figure 6. Differences in observed and simulated CFC-11 concentration (pmol/l) for the experiment with a source in (a) both the Labrador and Irminger Sea and a diffusivity of $3000 \text{ m}^2 \text{ s}^{-1}$, and (b) the Irminger Sea and a diffusivity of $1000 \text{ m}^2 \text{ s}^{-1}$.

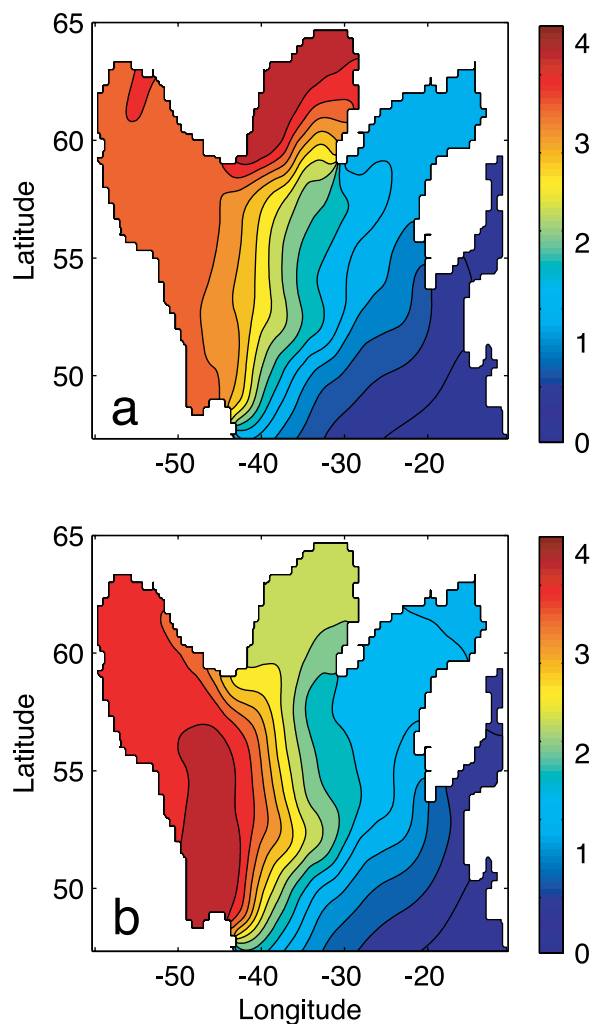


Figure 7. Simulated CFC-11 distributions (pmol/l) with uniform diffusivity ($1000 \text{ m}^2 \text{ s}^{-1}$) and a CFC-11 source in (a) the Irminger Sea, and (b) both the Labrador and Irminger Seas. The stream function is shown in Figure 1b, and is a constrained field calculated from a subset of the float data [Faure and Speer, 2005].

[18] In all these experiments with different stream functions, differences in CFC-11 concentration compared to observations are large in the southeastern corner of the basin, and comparatively small in the Labrador Sea. With both sources active, there are also large differences in the Irminger Sea. This pattern was also present in the original experiments with the unconstrained mean stream function, although in those cases the differences were slightly lower. Clearly, the model-data misfit is sensitive to relatively small changes in the circulation that are more or less consistent with the uncertainty in the float-based stream function.

3.4. Constraints on the Diffusivity

[19] Figure 8a shows results for each set of experiments for several diffusivities. Diffusivities less than $500 \text{ m}^2 \text{ s}^{-1}$ produce results that compare poorly with observations. Higher diffusivities give broadly similar χ^2 values with little sensitivity to large diffusivity despite the fact that the resulting solutions are unrealistically smooth. The χ^2 values

therefore mostly reflect the large scale CFC-11 pattern with high concentration in the northwestern part of the domain, decreasing toward the southeast. To further constrain the diffusivity, we explore the spatial correlation as a function of separation in the CFC-11 data and simulated fields (Figure 8b). The correlation coefficients among the different experiments all follow the same downward trend for separations less than 1500 km, but for larger separations they start to diverge. The curves for the data and simulations with diffusivity $\leq 2000 \text{ m}^2 \text{ s}^{-1}$ all cross the line of zero correla-

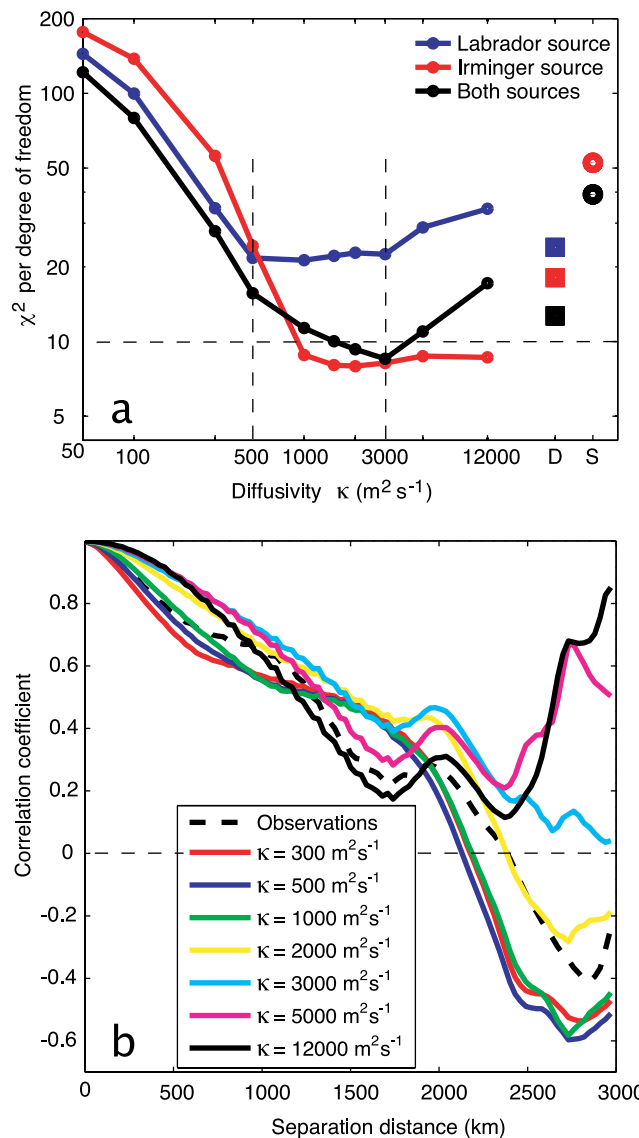


Figure 8. (a) Values of χ^2 in experiments with increasing uniform diffusivity. Squares on the right hand side marked with D on the x axis are χ^2 values for experiments with spatially varying diffusivity from Straneo *et al.* [2003]. Circles marked with S on the x axis are χ^2 values for experiments with the stream function shown in Figure 1b. The axes are logarithmic. (b) Spatial correlation coefficients as a function of separation distance for experiments with uniform diffusivity and CFC-11 sources in both the Labrador and Irminger Seas.

tion at separations of 2100–2400 km, but the curves for experiments with higher diffusivity never cross zero. Diffusivities less than $3000 \text{ m}^2 \text{ s}^{-1}$ therefore give the best comparison with observations. Diffusivities greater than this value give simulated CFC-11 fields that are qualitatively too smooth. The smaller scales present for diffusivity $<3000 \text{ m}^2 \text{ s}^{-1}$ do not fit the data very much better, however, because the χ^2 values are not much worse (Figure 8a).

[20] For each source configuration, experiments are also performed with the spatially-varying diffusivity fields from *Straneo et al.* [2003] (for example, Figure 3d). The impact on χ^2 is rather small, however, with just minor differences from the uniform $1000\text{--}3000 \text{ m}^2 \text{ s}^{-1}$ diffusivity experiments (Figure 8a). In this sense, the spatial field of diffusivity is not strongly constrained by the CFC-11 data.

3.5. Sensitivity to Tracer Source

[21] Finally, we address the sensitivity of our results to the CFC-11 source. The source regions shown in Figure 1 are reasonable choices based on the locations of deep winter convection. Nevertheless, convection to depths below the upper density surface for LSW occurs over a much broader area in the Labrador Sea, about $500 \text{ km} \times 600 \text{ km}$ [*Lilly et al.*, 1999]. We find that increasing the source area decreases the χ^2 values: For the Labrador Sea source χ^2 drops from 22 to 15 then 13 as the source area increases by factors of 30 and 90 over the original experiment. The overall pattern of model CFC field is qualitatively similar in these experiments. Similarly, in an experiment where both Labrador and Irminger sources are increased to fill almost all of these basins we find that the χ^2 values improve from 11 to 6.

[22] These results show that the CFC field is sensitive to the source area. A similar improvement can be obtained by using the original source area and an artificially-enhanced diffusivity in the Labrador Sea, however, using both sources and a spatially-variable diffusivity that peaks at $4000\text{--}5000 \text{ m}^2 \text{ s}^{-1}$ in the Labrador and Irminger Seas we achieve a χ^2 value of 3.7, reduced from 8.5 with a constant diffusivity of $3000 \text{ m}^2 \text{ s}^{-1}$. This result is consistent with the results on increasing source area because it also shows that CFC dispersal from the sites of injection has an important impact. These processes are beyond the scope of our model, however. They occur at, or below, the resolution of the float-based flow field and the CFC data and therefore constraining these processes is very difficult with these data and model.

4. Discussion

[23] We have used the 1996–2003 average float-based circulation field estimated by *Faure and Speer* [2005] in an advective-diffusive numerical model to simulate the mid-depth spreading of CFC-11 in the subpolar North Atlantic and compared to 1996–1998 average CFC-11 data from *Rhein et al.* [2002]. The main question is: Can the float-based velocity field be reconciled with the CFC-11 measurements taking into account the errors in the gridded CFC data and, crudely, the float-based circulation? The best fit we have found in a realistic configuration has a χ^2 value of 8.0 and there are many cases with values less than 10. By this measure, the CFC fields predicted by the float-based flow are close to being consistent with the CFC data, but do not fit in a satisfactory

way. Experiments using different stream functions clearly show that relatively small changes in the circulation and conditions in the CFC source areas significantly affects the values of χ^2 . This suggests that the problem of inferring a unique CFC-11 source pattern or eddy diffusivity is under-determined. Indeed, the best fit simulations include only an Irminger Sea source of LSW, which is obviously unrealistic. We conjecture that a stream function that is simultaneously consistent with the float and CFC data would look similar to Figure 1a with differences that are within the range of the differences between the existing estimates.

[24] Model CFC-11 concentrations in the south-eastern corner of the domain are too low in all experiments. Error in the float circulation is the leading candidate to explain these discrepancies, but other possibilities exist too. For example, the model unrealistically omits a (relatively weak) CFC source in both the deep North Atlantic Current entering the domain from the southwest, and the Mediterranean Water entering from the south east. Another possible explanation is time-varying flow or CFC source, which have both been neglected in this analysis. The subpolar North Atlantic is known to have undergone substantial changes in both circulation and convective activity during this period, however [*Haine et al.*, 2008; *Häkkinen and Rhines*, 2004]. It is therefore unlikely that these CFC-11 data alone will be able to exert strong constraints on these changes (although there is clear evidence of CFC sequestration into different varieties of LSW since 1997; *Kieke et al.* [2006]). Finally, the time periods and vertical coverage of the float data and CFC data, while overlapping, do not exactly coincide.

[25] Nevertheless, useful constraints are exerted on the middepth horizontal eddy diffusivity (which accounts for processes with scales less than $100\text{--}200 \text{ km}$). On the basis of the values of χ^2 and the spatial correlation analysis we have found that values of $500\text{--}3000 \text{ m}^2 \text{ s}^{-1}$ give similar results that best reproduce the observed CFC-11 field. With weaker diffusivity, the CFC-11 concentration is too low in areas not reached directly by advective pathways, while stronger diffusivity leads to a smooth field with no subbasin scale variability. The range of isopycnal diffusivities that match the CFC data is consistent with previous studies that have estimated isopycnal diffusivities of $O(10^3) \text{ m}^2 \text{ s}^{-1}$ [e.g., *Cunningham and Haine*, 1995b; *Khatiwala et al.*, 2002; *Straneo et al.*, 2003]. Moreover, the experiments that include a Labrador Sea and an intermittent Irminger Sea source of CFC-bearing LSW give better fits than those with only a Labrador Sea source. This result is consistent with the idea proposed by *Pickart et al.* [2003], that LSW can be formed both in the Labrador and Irminger Seas. Finally, because a large subset of experiments with different diffusivities and CFC-11 sources give similar values of χ^2 , it is reasonable to expect that other trace substances with similar atmospheric source functions behave the same. In particular, the float-based circulation field may well give an accurate field of anthropogenic carbon through the subpolar North Atlantic Ocean.

[26] **Acknowledgments.** We thank V. Faure and K. Speer for kindly providing the float data, M. Rhein and D. Kieke for the CFC-11 data, and F. Straneo for the variable diffusivity fields. Careful reviewers helped improve an earlier version of this paper. Funding was provided by the National Science Foundation, grants OCE-0326670 and OCE-0136327.

References

- Azetsu-Scott, K., E. P. Jones, and R. M. Gershey (2005), Distribution of water masses in the Labrador Sea inferred from CFCs and carbon tetrachloride, *Mar. Chem.*, *94*, 55–66.
- Cunningham, S. A., and T. W. N. Haine (1995), On Labrador Sea Water in the Eastern North Atlantic. part II: Mixing dynamics and the advective-diffusive balance, *J. Phys. Oceanogr.*, *25*, 666–678.
- Faure, V., and K. Speer (2005), Labrador Sea water circulation in the northern North Atlantic Ocean, *Deep Sea Res., Part II*, *52*, 565–581.
- Fischer, J., and F. A. Schott (2002), Labrador Sea Water tracked by profiling floats - From the boundary current into the open North Atlantic, *J. Phys. Oceanogr.*, *32*, 573–584.
- Getzlaff, K., C. Böning, and J. Dengg (2006), Lagrangian perspectives of deep water export from the subpolar North Atlantic, *Geophys. Res. Lett.*, *33*, L21S08, doi:10.1029/2006GL026470.
- Haine, T., C. Böning, P. Brandt, J. Fischer, A. Funk, D. Kieke, E. Kvaleberg, M. Rhein, and M. Visbeck (2008), North Atlantic deep water formation in the Labrador Sea, recirculation through the subpolar gyre, and discharge to the subtropics, in *Arctic-Subarctic Ocean Fluxes*, edited by R. R. Dickson et al., pp. 653–701, Springer, Netherlands.
- Häkkinen, S., and P. B. Rhines (2004), Decline of subpolar North Atlantic circulation during the 1990s, *Science*, *304*, 555–559.
- Khawiwala, S., P. Schlosser, and M. Visbeck (2002), Rates and mechanisms of water mass transformation in the Labrador Sea as inferred from tracer observations, *J. Phys. Oceanogr.*, *32*, 666–686.
- Kieke, D., M. Rhein, L. Stramma, W. M. Smethie, D. A. LeBel, and W. Zenk (2006), Changes in the CFC inventories and formation rates of Upper Labrador Sea Water, 1997–2001, *J. Phys. Oceanogr.*, *36*, 64–86.
- Lavender, K. L., R. E. Davis, and W. B. Owens (2000), Mid-depth recirculation observed in the interior Labrador and Irminger Seas by direct velocity measurements, *Nature*, *407*, 66–69.
- Lilly, J. M., P. B. Rhines, M. Visbeck, R. Davis, J. R. N. Lazier, F. Schott, and D. Farmer (1999), Observing deep convection in the Labrador Sea during winter 1994/1995, *J. Phys. Oceanogr.*, *29*, 2065–2098.
- Marshall, J., A. Adcroft, C. Hill, L. Perelman, and C. C. Heisey (1997), A finite-volume, incompressible Navier Stokes model for studies of the ocean on parallel computers, *J. Geophys. Res.*, *102*, 5753–5766.
- Pickart, R. S., D. J. Torres, and R. A. Clarke (2002), Hydrography of the Labrador Sea during active convection, *J. Phys. Oceanogr.*, *32*, 428–457.
- Pickart, R. S., M. A. Spall, M. H. Ribergaard, G. W. K. Moore, and R. F. Milliff (2003), Deep convection in the Irminger Sea forced by the Greenland tip jet, *Nature*, *424*, 152–156.
- Rhein, M., J. Fischer, W. M. Smethie, D. Smythe-Wright, R. F. Weiss, C. Mertens, D. H. Min, U. Fleischmann, and A. Putzka (2002), Labrador Sea Water: Pathways, CFC-inventory and formation rates, *J. Phys. Oceanogr.*, *32*, 648–665.
- Schmitz, W. J. (1995), On the interbasin-scale thermohaline circulation, *Rev. Geophys.*, *33*, 151–173.
- Schmitz, W. J. (1996), *On the World Ocean Circulation*, vol. 1, *Some Global Features/North Atlantic Circulation*, Technical Report, Woods Hole Oceanographic Institution, Woods Hole, Mass.
- Schmitz, W. J., and M. S. McCartney (1993), On the North Atlantic circulation, *Rev. Geophys.*, *31*, 29–49.
- Straneo, F., R. S. Pickart, and K. Lavender (2003), Spreading of Labrador Sea Water: An advective-diffusive study based on Lagrangian data, *Deep Sea Res., Part I*, *50*, 701–719.
- Talley, L. D., and M. S. McCartney (1982), Distribution and circulation of Labrador Sea Water, *J. Phys. Oceanogr.*, *12*, 1189–1205.
- Walker, S. J., R. F. Weiss, and P. K. Salemeh (2000), Reconstructed histories of the annual mean atmospheric mole fractions for the halocarbons CFC-11, CFC-12, CFC-113, and carbon tetrachloride, *J. Geophys. Res.*, *105*, 14,285–14,296.
- Warner, M. J., and R. F. Weiss (1985), Solubilities of chlorofluorocarbons 11 and 12 in water and sea water, *Deep Sea Res., Part I*, *32*, 1485–1497.
- Yashayaev, I. (2007), Hydrographic changes in the Labrador Sea, 1960–2005, *Prog. Oceanogr.*, *73*, 242–276.

T. W. N. Haine and D. W. Waugh, Department of Earth and Planetary Sciences, Johns Hopkins University, 329 Olin Hall, 3400 North Charles Street, Baltimore, MD 21218, USA. (thomas.haine@jhu.edu)

E. Kvaleberg, Norwegian Naval Training Establishment, Tactics and Doctrine/METOC, P.O. Box 5 Haakonsværn, N-5886 Bergen, Norway. (ekvaleberg@mil.no)